論文 85-22-5-15

Two-Dimensional Simulation of MOS Transistors Using Numerical Method

수치해석 방법에 의한 2차원적인 MOS Transistor의 시뮬레이션에 관한 연구

鄭 泰 聖*, 慶 宗 旻*
(Tae Sung Jung and Chong Min Kyung)

要 約

다양한 채널 길이와 임의의 인가전압하의 MOS 트랜지스터를 2차원적으로 시 레이션 하기위한 프로그램(SOMOS)을 제작하였다. Poisson의 방정식에 대하여는 Newton 방법을, 연속방정식에 대하여는 발산정리를 이용하여 기본 수식들에 대한 유한차등법(FDM)에 따른 수식을 전개하였으며, 선형화된 수식의 해는 SOR 방법과 Gummel의 알고리즘을 이용하여 구했다. 하나의 동작상태의 소자를 시뮬레이션 하기위한 시간은 VAX 11/780 컴퓨터를 사용했을때 인가전압 상태에 따라 30초 내지 4분 정도가 소요되었다. 인가전압과 전위분포에 따라 자동적으로 생성되는 그리드는 비균일한 간격을 가지며 필요에 따라 자동적으로 개선된다.

Abstract

A two-dimensional numerical analysis program, called SOMOS (simulation of MOS transistors), has been developed for the simulation of MOSFET's with various channel lengths and bias conditions. The finite difference approximation of the fundamental equations are formulated using Newton's method for Poisson's equation and the divergence theorem for the continuity equation.

For the solution of the linearized equations, SOR (successive over relaxation) method and Gummel's algorithm have been employed. The total simulation time for one operating point is varying between 30 sec. and 4 min. on VAX 11/780 depending on bias conditions. The nonuniform mesh was generated and refined automatically to account for various bias values and the potential distributions.

I. Introduction

As the transistor dimensions shrink with the rapid technological advances in the field of semiconductor device processing, one is compelled to use the numerical models to retain the computational accuracy.

The first consistent simulation model incorporating the fundamental semiconductor transport equations was reported by Gummel for the bipolar transistor./1/ There followed a

*正會員, 韓國科學技術院 電氣 및 電子工學科
(Dept. of Elec. Eng., KAIST)

接受日字 : 1985年 5月 28日

flood of analogous work with refinements and improvements in one way or another. In this work, a computer program called SOMOS (simulation of MOS transistor) was developed, where the doping profiles are given as the starting point for solving the Poisson's equation and the continuity equation in two-dimensional finite-difference grid space.

The two dimensional equi-distance doping profile, which may be taken from the two dimensional process simulation result for the source and drain, is used for more accurate estimation of the lateral diffusion. SUPREM/ 6/, the Stanford University Process Engineering Model program, or DIFSIM /4/ can be used to give the one dimensional equi-distance doping profile for the simulation of the channel implanted MOS transistors.

Since the mesh allocation strongly affects the convergence characteristics of system equations, an adaptive grid system with varying mesh size was employed.

Finally, several electrical characteristics of the MOS transistor was shown for demonstration purpose.

II. Model Description

In this chapter the fundamental semiconductor equations, the necessary physical assumptions and some models for a two dimensional numerical analysis of MOSFET will be discussed.

1. Basic Semiconductor Equations

The electrical behavior of electronic devices is governed by electromagnetic field equations. It is known that for silicon devices with dimension of a few microns and for frequency up to 10^{10} Hz, the quasi-static approximation of the field equations is valid. These equations are contained in the following five equations,

$$\mathrm{div\,grad}\ \psi = -q\,(p-n+ND^{+}-NA^{-}) \qquad (1)$$
$$\mathrm{div}\ J_n - q\,(\partial n/\partial t) = q\,R \qquad (2)$$
$$\mathrm{div}\ J_p + q\,(\partial p/\partial t) = -q\,R \qquad (3)$$
$$Jn = -q\,(\mu_n\, n\ \mathrm{grad}\ \psi - D_n\ \mathrm{grad}\ n) \qquad (4)$$
$$Jp = -q\,(\mu_p\, p\ \mathrm{grad}\ \psi + D_p\ \mathrm{grad}\ p) \qquad (5)$$

where all the symbols have their conventional meanings.

Eq. (1) is Poisson's equation for the electrostatic potential. Eq. (2), (3) are called the continuity equations.

This set of equations was first given in closed form by Van Roosbroeck /7/ in 1950.

2. Model Equations with Its Chosen Assumptions

A number of assumptions have been introduced into the model to simplify the computation without a considerable loss of accuracy.

a. Only steady-state solutions are sought.

$$\partial n / \partial t = 0 \qquad (6)$$
$$\partial p / \partial t = 0 \qquad (7)$$

b. Dielectric constant of silicon and oxide are isotropic.

c. Total ionization of the donor and acceptor impurities is assumed.

$$C = ND^{+} - NA^{-} = ND - NA \qquad (8)$$

d. Degeneracy phenomena will not be considered.

$$n_i = \mathrm{const} \qquad (9)$$

e. Majority carrier current is neglected

$$Jp = 0 \text{ (for n-channel MOS)} \qquad (10)$$
$$Jn = 0 \text{ (for p-channel MOS)} \qquad (11)$$

f. The operating temperature throughout the entire transistor is constant.

g. The carrier distribution is described by Boltzman statistics.

$$n = n_i\, e\,(\psi-\phi_p)/V_T \qquad (12)$$
$$p = n_i\, e\,(\phi_p-\psi)/V_T \qquad (13)$$

h. The Einstein relation is assumed to be valid.

$$Dn = \mu_n\, V_T \qquad (14)$$
$$Dp = \mu_n\, V_T \qquad (15)$$

1) All Contacts are Assumed to be Ohmic. The space change vanishes at the contacts, and the carrier distribution is in the thermal equilibium.

A normalization into dimensionless form is carried out following De Mari /2/.

From the chosen assumptions found and those normalization factors the model is reduced to the following nonlinear system

of partial differential equations:

For the n-channel devices:

$$\text{div grad } \psi = e\psi \cdot \phi n - e\phi P - \psi - C \quad (16)$$

$$\text{div } J_n = R$$

$$Jn = -\mu_n \, n \text{ grad } \phi_n$$

$$\phi_p = \text{const (that is, } Jp=0).$$

For p-channel devices

$$\text{div grad } \psi = e^{\psi} - {}^{\phi n} - e^{\phi} p - C \quad (17)$$

$$\text{div } J_p = -R$$

$$J_p = -u_p \, p \text{ grad } \phi_p$$

$$\phi_n = \text{const (that is, } J_n=0)$$

Eq. (16) and (17) actually describe a coupled system of two nonlinear differential equations.

3. Physical Parameters

a. The intrinsic carrier concentration is modeled as being only temperature dependent.

$$n_i = 3.88 \times 10^{16} \times T^{1.5} \times e^{-7000/T} \text{ cm}^{-3} \quad (18)$$

where T denotes the temperature in degree Kelvin.

b. Shockly-Read-Hall model is used for the description of thermal generation.

$$R_{SRH} = \frac{p\,n - n_i^2}{\tau_p(n+n_i) + \tau_n\,(p+n_i)} \quad (19)$$

where τ_p, τ_n denote the carrier lifetime. The generation rate term due to the impact or avalanche ionization mechanism and band-to-band recombination terms are neglected in this work.

c. Doping profile

The doping profile is the starting and the most important parameter for the simulation of the transistors.

There are two types of doping profile in SOMOS.

One is a two-dimensional doping profile in uniform grid for the source and the drain, the other is one dimensional doping profile, in uniform grid with the grid size basically different from that of 2-D profile, for the channel-implanted transistors.

The 1-D doping profiles can be given by one of the available process simulators, such as SUPREM /6/, DIFSIM (one-dimensional process simulation program developed at KAIST) /4/. Likewise, the 2-D profile can be obtained via 2-D process simulators such as PRECISE, which is a 2-D version of DIFSIM /5/.

d. Carrier mobility.

Carrier mobility is degraded by various scattering mechanisms. First of all, carriers are scattered by defects resulting in the relatively high bulk mobility.

This lattice mobility is reduced by additional coulomb scattering at ionized impurity atoms.

Caughey and Thomas /8/ have given the following empirical expression fitting experimental data for carrier mobilities:

$$\mu(NT) = \mu_{min} + \frac{\mu_{max} - \mu_{min}}{1 + (NT/Nref)^{\alpha}} \quad (20)$$

where NT= ND + NA is the total doping concentration.

Fitting Eq. (20) to more recent measurements leads to the coefficients given in Table 1.

Table 1. Mobility parameters

	μ max $(cm^2v^{-1}s^{-1})$	μ max $(cm^2v^{-1}s^{-1})$	Nref (cm^{-3})	α —
electron	1360	92	1.3×10^{17}	0.91
hole	520	65	2.4×10^{17}	0.61

Measurements have shown that for high excess carrier densities mobility is further reduced by electron-hole scattering.

Following /9/, the experimental data can be fitted by replacing the total doping concentration in (20) by the expression

$$NT = 0.34\,(ND+NA) + 0.66\,(\bar{n}) \quad (21)$$

with $\bar{n} = p + n$ and using the coefficients of Table 1.

The field dependence measured in low-doped material can be taken into account by the expression

$$\mu(N,\bar{n},E) = \mu(N,\bar{n})[1 + (\mu(N,\bar{n})E/V_{max})^{\beta}]^{-1/\beta} \quad (22)$$

with $\beta n=2$ and $\beta p=1$ resulting in doping-independent limiting drift velocities of

$$V_{max,n} = 1.1 \times 10^{7} \text{cm/s} \quad (23)$$

and $V_{max,p} = 9.5 \times 10^{6}$ cm/s

Another important fact in MOSFET simulation is that the channel mobility is further reduced by surface scattering of carriers due to surface roughness.

Following /10/, this effect can be taken into account by splitting the electric field strength into two components, E_{11} and $E_{\perp}$, which are longitudinal and transversal to the direction of current flow.

In this work, the E term used in Eq. (22) represents E_{11} and the resulting mobility is further reduced by

$$u(N,E_{11}, E)=u(N,E_{11})(1+\alpha E_{\perp})^{-1/2} \quad (24)$$

with $\alpha_n = 1.54 \times 10^{-5}$ cm/V and $\alpha_p = 5.35 \times 10^{-5}$ cm/V.

III. Numerical Treatment

In order to transform the physical model of a semiconductor device into a numerical model, fundamental equations are linearized to ease the discretization process.

Through this chapter the recurrent FDM (Finite Difference Method) equations are formulated with the applicable boundary conditions.

1. Solution Method

Although the system of equations examined in the following is exclusively for NMOS transistor an extension to handle PMOS transistor is obvious because the equations for the PMOS transistor are structually identical to those of NMOS transistor.

For the purpose of clarity and for prevention of numerical over6 underflow, this system is generally represented in its normalized form.

$$\text{div grad } \psi = n - p - C \quad (25)$$

$$\text{div}(u_n \, n \, \text{grad } \phi_n) = \frac{1 - n p}{\tau_p(n+1)+\tau_n(p+1)} \quad (26)$$

with : $n = e^{\psi - \phi_n}$ $\quad p = e^{\phi_p - \psi}$

ϕ_p = const $\quad C = C(x,y)$

$\mu_n = \mu_n(x,y)$ $\quad \tau_n$ = const

τ_p = const

For the solution of this system, 2N nonlinear equations have to be solved, where N is the number of grid points and usually lies between 300 and 4000 in the two-dimensional case. Therefore, it is of great importance to choose an efficient algorithm to minimize the computational cost.

A simple choice is that one treats eq. (25) and eq.(26) separately in a decoupled manner and solving one after the other repetitively. First, Poisson's equation is solved assuming known quasi-Fermi level. Next comes the continuity equation with the potential given from the solution of Poisson's equation.

This sequence is iteratively repeated until self-consistent values of the desired accuracy for all unknown variables are obtained/1/.

This approach is advantageous for multi-dimensional simulations as it saves storage and converges quite well especially if the coupling between the two equations is weak.

This relatively simple implementation of the decoupled method has to be paid for by its possible slow convergence especially if eq. (25) and eq. (26) are strongly coupled.

These convergence problems can be overcome mathematically by solving eq. (25) and eq. (26) simultaneously rather than alternatively. Although this simultaneous Newton method is advantageous from a purely mathematical viewpoint, it is more involved with regard to storage requirements. Some characteristics of these two methods are compared in /11/.

In this work, we chose the conventional decoupled method for no other obvious reason than simplicity.

Poisson's equation is considered as a nonlinear equation in Eq. (25) while ϕ_n, ϕ_p are known.

One first applies the Newton-like formulation for the linearization of Poisson's equation and after simple algebraic transformation,

$$\psi^{k+1} = \psi^k + \delta \tag{27}$$

$$\text{div grad } \delta - \delta(n+p) = n - p - C - \text{div grad } \psi^K + O(\delta^2)$$

with $n = e^{\psi - \phi_n}$

$p = e^{\phi_p - \psi}$

In above equations, ψ^k denotes the value of ψ after k-th iteration.

Because of the exponential terms in Poisson's equation, some authors /12/,/13/ have proposed the damping of the corrective potential term, δ, in order to prevent an eventual overshooting of Newton procedure.

This can be done in the following manner /12/:

evaluate for each element

$$\delta_i = \begin{cases} \delta_i, & \text{for } |\delta_i| \leqslant 1 \\ \text{sgn}(\delta_i)\, |\delta_i|^{1/5}, & \text{for } 1 < |\delta_i| < 3.7 \\ \text{sgn}(\delta_i)\, \ell_n |\delta_i|, & \text{for } |\delta_i| \geqslant 3.7 \end{cases} \tag{28}$$

The relevant literature offers a wide spectrum of similar variants /13/.

The linearization of the continuity equation can be achieved by the analogous way as was explained for Poisson's equation, but this linearization can, in general, be omitted because of its weak nonlinearity.

2. *Discretization of Poisson's Equation and the Continuity Equation*

In this work the five-point discretization scheme was employed, which was also preferred by many workers in their two dimensional modeling.

One substitutes the differential equation on each inner point (i, j) (see Fig. 1) through a difference equation. Fig. 2 shows the basic geometry for the MOSFET model being used in SOMOS.

Eq. (25) is an elliptic differential equation. Care has to be taken only with the discretization of the interface (line BE in Fig. 2),

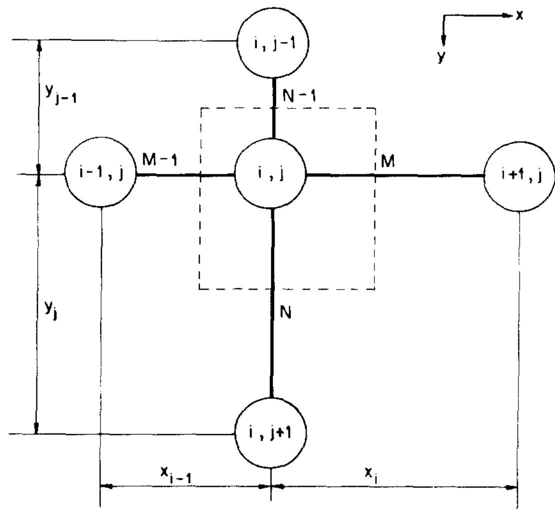

Fig. 1. Node Scheme for finite difference method.

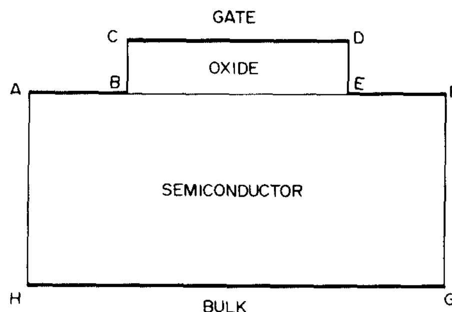

Fig. 2. Domain for MOSFET simulation.

because of the discontinuity of the space charge.

By applying the central differencing the Poisson's equation and the continuity equation were formulated in two-dimensional finite-difference grid space in a similar way as that of the original one-dimensional work by Scharfetter and Gummel /14/.

3. *Boundary Conditions*

First we discuss the boundary conditions for Poisson's equation on the geometrical model shown in Fig. 2. At the contacts (AB: Source, CD: Gate, EF: Drain, GH: Bulk) which are assumed to be ohmic, the potential is kept to

the value of the applied bias voltage plus the built-in potential.

At the vertical boundaries (AH, CB, DE, FG) electric field perpendicular to the surface has to vanish.

At the interface(BE), the electric potential has to satisfy the law of Gauss.

$$\epsilon_{ox} \left.\frac{\partial\psi}{\partial y}\right|_{oxide} = \epsilon_{si} \left.\frac{\partial\psi}{\partial y}\right|_{silicon} \qquad (31)$$

The boundary conditions of the continuity equation are simple as was the case for Poisson's equation.

At all contacts (AB: Source, EF: Drain, GH: Bulk) the carrier density is kept to the value of the doping concentration. At the interface(BE), no current component in y direction is allowed. At the vertical bounderies (AH, FG) the lateral current component has to vanish.

4. *Grid and Initial Solutions*

Careful attentions must be given to the selection of the grid points in order to minimize the discretization error which has a very strong influence upon the convergence characteristics.

It is impossible to choose an equidistant grid, because too many grid points would require undesirable memory space and computation time.

Because of the above mentioned reasons, a grid with unequal spacing is used, which will then be checked in a certain phase of the solution procedure.

Initial grid generation is based on the doping concentration and given bias conditions. Refined grid is generated, automatically, to satisfy the requirement that the absolute potential difference between two adjacent grid points are within the specified range.

Two-dimensional potential distribution which is used as the initial solution is generated as was done in MINIMOS/3/.

For the simplicity and the easy programming, initial carrier distribution for a given bias is assumed to be equal to that of thermal equilibrium.

IV. Typical Application Example

In this chapter some typical application examples will be presented. The appropriate example as an application of two dimensional modeling would be the analysis of the influence of an ion-implantation upon short channel transistors.

For that purpose, two different transistors I and II were simulated whose data are declared in SOMOS input statement table 2.

For the user's convenience, input statements and syntax used in MININOS /3/ are retained in SOMOS except some modifications.

Transistor I and II have identical input statements but the channel was implanted in transistor II. Input statement sets are listed in table 2.

Table 2. Input Statement Sets for SOMOS

```
*APPLICATION EXAMPLE DEVICE I AND II*
DEVICE  CHANNEL=N GATE=NPOLY TOX=
    350E-8 W=10E-4 L=2E-4
BIAS    UD=3 UG=0 US=0
OUTPUT  DC=Y PSI=Y CC=Y MOB=Y
END
```

The first line is a title. The further syntax is based upon a keyword-parameter-value structure and is completely format free.

"DEVICE" key describes the type and geometry of the MOSFET. "BIAS" key describes the operating point of the MOSFET.

"OUTPUT" key describes the parameters required to be written in the output file.

Several values for error control and the number of iterations are tested. Here, the system equations are solved by the SOR method with the condition of max (1delta variatel) $\leqslant 1 \times 10^{-5}$

The number of Newton's iteration within Poisson's equation is usually between 3 and 6. It is believed that this number may depend on the damping scheme. Overall procedure is stopped when the variation of the electrostatic potential is less than V_T, the thermal voltage. The doping density distribution are shown in Fig. 3. Doping data for source and drain are obtained from PRECISE/5/. SUPREM /6/ was used for channel implant profile in the transistor. In these figures, the drain contacts are on

the right-hand side. The effective channel length is reduced by the lateral diffusion to about 1.6 um.

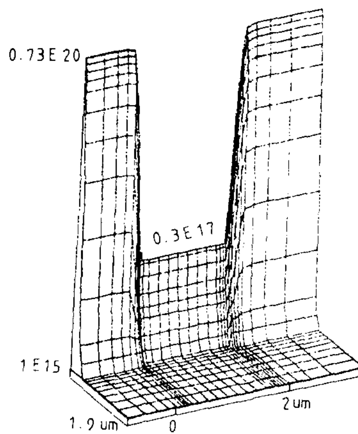

Fig. 3 Total doping profile in the transistor II.

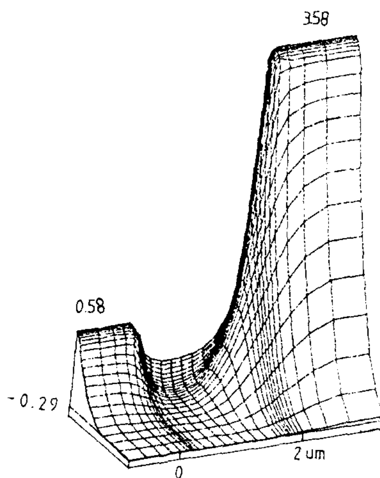

Fig. 4. Potential distribution in the transistor II.

Fig. 4 shows the distribution of the electrostatic potential in the transistor. The zero potential point corresponds to the mid-gap level in the energy band diagram. In the depletion region of the reverse biased drain/bulk diode, the potential falls monotonically, and it is nearly constant in the highly doped source and drain region.

Fig. 5 shows the electron concentration profile. As was expected, the surface concentration is depressed because of the channel implantation. Fig. 6 shows the mobility distribution. In the highly doped source/drain region, the mobility is very small because of the impurity and carrier scattering. Under the source region, the mobility immediately increases to its bulk value, but under the drain region the mobility reduction due to the strong field in the reverse biased drain/substrate diode is observed. The mobility in the channel region falls off monotonically along the surface. In the normal direction, the mobility parallel to the surface is reduced by the surface scattering.

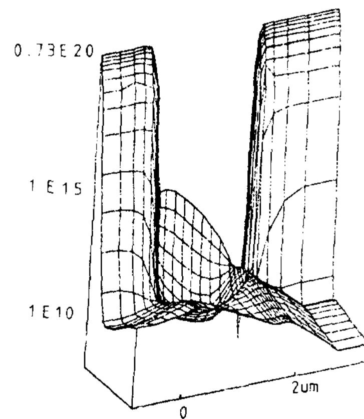

Fig. 5. The electron distribution in the transistor II.

V. Conclusion

In this paper, we described a program, SOMOS, for the two dimensional numerical simulation of the planar NMOS transistors.

This program includes the SRH recombination model and the mobility dependences on the impurity atom density, carrier concentration, velocity saturation and the channel surface state.

The finite difference formulations for the basic semiconductor equations are explained. For the solution of the system equations, the SOR method has been employed.

The main motivation for the development of this program was to gain physical understanding of MOS transistor operation and to provide both designers and technologists with a conveniant and accurate MOSFET simulator.

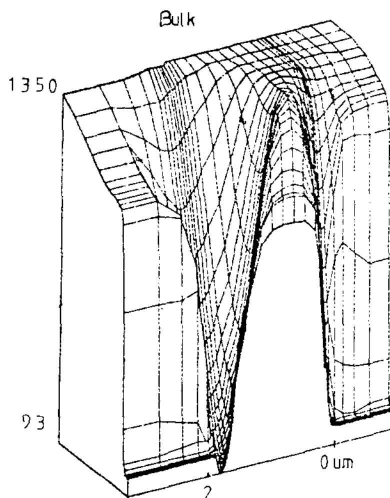

Fig. 6. Mobility distribution in the transistor II.

It is found that the drain currents that are calculated from the different points of grid within the channel region have somewhat different values and the efforts to obtain I-V characteristic curves for various drain and gate bias have failed.

It is expected that another accurate and efficient simulation would be possible by adopting such algorithms as "decoupled method" and SLOR, SIP /15/, ICCG /16/, etc.

References

[1] H.K. Gummel, "A self consistent iterative scheme for one dimensional steady state transistor calculations," *IEEE Trans. Electron Devices,* vol. ED-11, pp. 445-465, 1964.

[2] A. De Mari, "An accurate numerical Steady-State One-Dimensional Solution of the P-N Junction," *Solid-State Electron.,* vol. 11, pp. 33-58, 1968.

[3] S. Selbeherr, A. Schutz, H.W. Potzl, "MINIMOS-A Two-Dimensional MOS Transistor Analyzer," *IEEE Trans. Electron Device,* vol. ED-27, pp. 1540-1550, 1980.

[4] H.C. Oh, C.M. Kyung, "Numerical Evalution of Impurity Profile in Silicon," *J. KIEE,* vol. 21, no. 6, pp. 17-26, 1984.

[5] Y.Y. Yang, H.C. Oh, C.M. Kyung, *Characterization of Two-Dimensional Impurity Profile in Semiconductor Using Direct Method.* Presented at the int'l Electronic Devices and Materials Symposium, Taiwan, ROC, Sept., 1984.

[6] C.P. Ho, S.E. Hansen, "*SUPREM III - A Program for Integrated Circuit Process Modeling and Simulation.* SEL 83-001 Stanford Electronics Labs, Stanford University, July 1983.

[7] W.V. Van Roosbroeck, "Theory of flow of electrons and holes in germanium and other semiconductors," *Bell Syst. Tech. J.,* vol. 29, pp. 560-607, 1950.

[8] D. M. Caughey and R.E. Thomas, "Carrier mobilities in silicon empirically related to the doping and field," *Proc. IEEE,* vol. 55, pp. 2192-2193, 1967.

[9] W. Anheier and W.L. Engl, *Numerical analysis of gate triggered SCR turn-on transients,* in IEEE IEDM Dig. Tech. Papers (Washington D.C.), pp. 303A-3030, 1977.

[10] K. Yamaguchi, "Field-dependent mobility model for two dimensional numerical analysis of MOSFET's," *IEEE Trans. Electron Device,* vol. ED-26, pp. 1068-1074, 1979.

[11] E. M. Buturla, P.E. Cotrell, "Simulation of Semiconductor Transport Using Coupled and Decoupled Solution Techniques," *Solid-State-Electronics,* vol. 23, pp. 331-334, 1980.

[12] B.W. Brown, B.W. Lindsay, "The Numerical Solution of Poisson's Equation for Two-Dimensional Semiconductor Device," *Solid-State-Electron,* vol. 19, pp. 991-882, 1976.

[13] S. Selberherr, *English Translation of Two Dimensional Modeling of MOS Transistors.* The Original Paper is Ph.D. Dissertation Thesis, Technical University of Vienna, Austria. Translated by Semiconductor Physics, Inc. 639 Meadow Grove place Escondido, CA 92027, 1982.

[14] D.L. Scharfetter, H.K. Gummel, "Large-signal analysis of a silicon read diode oscillator," *IEEE Trans. Electron Devices,* vol. ED-16, pp. 64-77, 1969.

[15] H.L. Stone, "Iterative solution of implicit approximation of multidimensional partial differential equations," *SIAM, J. NUM. Anal.*, vol. 5, pp. 530-558, 1968.

[16] J.A. Meijerink and H.A. Van der Vorst, "An iterative method for linear systems of which the coefficient matrix is a symmetric M-Matrix," *Math. of Computation*, vol. 31, no. 137, pp. 148-162, 1972.